Current Research in Food Science 5 (2022) 2125–2134

Contents lists available at ScienceDirect

Current Research in Food Science

journal homepage: www.sciencedirect.com/journal/current-research-in-food-science

Effects of *Ilisha elongata* protein, soy protein and whey protein on growth characteristics and adhesion of probiotics

Guoyan Liu [b], Meng Chu [b], Shiying Nie [a], Xin Xu [b,**], Jiaoyan Ren [a,*]

[a] School of Food Science and Engineering, South China University of Technology, Guangzhou, 510641, China
[b] College of Food Science and Engineering, Yangzhou University, Yangzhou, 225127, China

ARTICLE INFO

Handling editor: Dr. Quancai Sun

Keywords:
Ilisha elongata proteins
Soy proteins
Whey proteins
Lactobacillus plantarum 45
Proliferation
Adhesion

ABSTRACT

The effects of different food source proteins on the growth characteristics and intestinal adhesion of *Lactobacillus plantarum* 45 (LP45) were investigated by adding *Ilisha elongata* protein, soy protein and whey protein to the probiotic bacteria in vitro and using a probiotic adhesion model based on mouse intestinal tissues. *Ilisha elongata* protein and soy protein significantly reduced the growth time of LP45 and increased the total number of colonies fermented by LP45; whey protein only reduced the growth time of LP45; the effect of the three food source proteins on the acid production capacity of LP45 was small. These showed that the three food-derived proteins promoted the proliferation and adhesion of probiotics in the intestine, which were beneficial to the active role of intestinal probiotics and improved the intestinal microenvironment.

1. Introduction

Dietary nutrients are essential not only for human health, but also for the health and survival of the trillions of microorganisms that inhabit the human gut (Shoaie et al., 2015). Dietary nutrients are key regulators of the relationship between humans and their microbiota, and dietary intake appears to be a major short-term and long-term regulator of gut microbiota structure and function, based on studies in animals and humans (Schroeder et al., 2017). There is growing evidence that diet has a broad impact on human health and disease, and the gut microbiome is the intersection of humans and their gut health (Gentile and Weir, 2018).

Every major macronutrient and many micronutrients have been shown to alter gut microbiota (Zhang et al., 2011; Mastrocola et al., 2018). The researchers investigated the prebiotic effects of dietary carbohydrates on gut probiotics more, because gut microbes have a large number of carbohydrate-degrading enzymes. Some indigestible carbohydrates are prebiotics, such as fructooligosaccharides, inulin, etc. In addition to oligosaccharides, proteins, hydrolysates and peptides have also been shown to be prebiotics that promote the growth of probiotics (Zhang et al., 2020).

Since some probiotics cannot directly utilize exogenous proteins, they must degrade exogenous proteins or peptides to ensure normal growth and metabolism. Therefore, in an environment where protein constitutes the main nitrogen source, the proteolytic system must play an active role (Pritchard and Tim, 1993). The study found that the mechanism of action of protein on probiotics includes providing essential amino acids for probiotics, improving the resistance of strains to acidic environments, promoting amino acid and protease activity and other beneficial effects on probiotics (Juillard et al., 1995).

Probiotics need to experience the strong acidic environment of the stomach to reach the intestine, and there is abundant bile in the small intestine, so acid resistance and bile salt resistance are one of the criteria for probiotic screening (Han et al., 2021). Secondly, an important prerequisite for the colonization of probiotics in the intestinal tract is that probiotics can adhere and proliferate in the intestinal tract (Alp and Kuleaşan, 2019). The proliferation of probiotics requires nutrient supply, and protein and polysaccharide can be used as growth promoting factors for probiotics. Adherence and colonization of probiotics in the intestine is the basis for their physiological effects. Probiotic adherence helps to maintain the normal intestinal flora structure, maintain the morphological and functional integrity of the intestinal mucosa, enhance the signal communication between probiotics and intestinal epithelial cells, and inhibit the colonization of harmful bacteria in the

* Corresponding author. School of Food Science and Engineering, South China University of Technology, Wushan Rd. 381, Guangzhou, 510641, China.
** Corresponding author.
E-mail addresses: yzufsff@163.com (G. Liu), 2361338382@qq.com (M. Chu), nsymasaki1224@163.com (S. Nie), xuxin@yzu.edu.cn (X. Xu), jyren@scut.edu.cn (J. Ren).

https://doi.org/10.1016/j.crfs.2022.10.024
Received 15 June 2022; Received in revised form 8 September 2022; Accepted 22 October 2022
Available online 4 November 2022

intestine (Thomas and Versalovic, 2014).

Prebiotics such as inulin and oligosaccharides are often used as dietary supplements to improve intestinal homeostasis due to their beneficial effects on improving colonization resistance and regulating the intestinal microenvironment. However, little is known about the functional interaction between food-derived proteins and intestinal probiotics, and it is noteworthy that whether the proteins also have similar probiotic effects. Therefore, this study aimed to investigate the effects of *Ilisha elongata* proteins (IeP), soy protein (SP), and whey protein (WP) on the growth characteristics and adhesion of intestinal probiotics.

2. Materials

2.1. Materials and reagents

IeP is homemade by the laboratory, SP and WP are provided by Guangzhou State Good Biotechnology Co,. The protein content of *Ilisha elongata* protein was 65.66% by Kjeldahl nitrogen determination. The protein content of SP and WP is 99% respectively. *Lactobacillus plantarum* 45 (LP45) were preserved by our laboratory. Beef extract, yeast extract, peptone, Tween-80, triammonium citrate, manganese sulfate monohydrate, magnesium sulfate heptahydrate, agar and glucose were purchased from Bioengineering (Shanghai) Co. Pentobarbital and glutaraldehyde were purchased from Shanghai Maclean Biochemical Technology Co. Crystalline violet was purchased from Shanghai Yuanye Biotechnology Co. All other chemical reagents and solvents used in the experiments were of analytical reagent grade.

2.2. Determination of structural properties of proteins

Protein molecular weight analysis: Take food-derived protein, configure protein concentration of about 2 mg/mL, add appropriate amount of 5 × spiking buffer according to the protein content of the sample to be measured, make the final concentration of sample protein 0.5–2.0 mg/mL, mix well, heat in boiling water bath for 3–5 min, remove and cool, centrifuge at 10, 000 rpm for 15 s, take the supernatant and set aside. The SDS-PAGE gel electrophoresis conditions were: 12% for the separation gel and 5% for the concentration gel, and the gel was stained for 2 h with Coomassie Brilliant Blue R-250 staining solution (0.5 g Coomassie Brilliant Blue R-250 dissolved in a mixture of methanol and glacial acetic acid (80 mL/20 mL)) after electrophoresis. The bands were photographed with a gel imaging system.

Scanning electron microscopy analysis: Firstly, the conductive double-sided adhesive was attached to the carrier table, and the protein samples were taken and pasted on the conductive adhesive and sputter coated with pure gold, and then SEM imaging was used to observe the protein microscopic morphology with a magnification of 1, 000 times.

Infrared spectroscopy analysis: Take about 1.0 mg of protein sample powder and place it on the carrier table, start pressing the tablet, slowly increase the strength until there is no large fluctuation in the infrared spectrogram, stop pressing the tablet, and use an infrared spectrometer to scan in the wavelength range of 600–4, 000 cm^{-1} to obtain the infrared spectral scan results of the protein.

Circular dichroism: Referring to the determination method studied by Deng et al. (Deng et al., 2019), food-derived proteins were prepared in deionized water to a solution of 1.0 mg/mL, pH adjusted with 1.0 mol/L HCl/NaOH (2.0–10.0), and scanned in the wavelength 190–250 nm (far UV). After scanning, data processing of the spectra was performed with CD Tool software to calculate the content of protein α-helix, β-fold, β-turn and irregularly coiled structures.

2.3. Determination of amino acid composition of proteins

The amino acid composition was determined according to the method studied by Deng et al. (Deng et al., 2019). The ampoule was carefully weighed 15.0 mg of protein sample and added to the ampoule to prevent hanging as much as possible, then 10.0 mL of 6.0 mol/L HCl was added. The ampoule was nitrogen blown and exhausted, and sealed with an alcoholic blowtorch, 3–4 drops of phenol were added, liquid nitrogen was frozen for 3 min, nitrogen blowing-evacuation was repeated 3 times, the cap was screwed tightly and placed in an oven at 110°C for 22 h. After the acid hydrolysis was cooled, the hydrolyzed After the acid hydrolysis was cooled, the hydrolyzed sample was filtered through filter paper into a 25 mL volumetric flask, the filter paper was washed three times, and the solution was finally volume fixed to the 25 mL scale. Aspirate 1 mL of the solution into a drying dish, dry it in an oven at 60 °C, add water to re-dissolve it after drying and repeat drying twice, and dry it until only traces of solid remain. Finally, the freeze-dried sample was re-dissolved, and 2 mL of 0.02 mol/L dilute hydrochloric acid was drawn into the sample bottle after dissolving the deacidified sample and filtered into the injection bottle using 0.22 μm filter head, and detected on the machine. The amino acid composition of the supernatant was analyzed by automatic amino acid analyzer L-8900. Quantification was performed by external standard method using standard amino acid solutions.

2.4. Determination of probiotic growth characteristics

The probiotic lyophilized powder was activated continuously for 3 generations, inoculated into MRS medium, and incubated at 37°C, 200 rpm overnight. Then inoculate 1% into MRS-protein medium. After setting up the grouping, 200 μL of bacterial solution was added to each well in a 96-well plate, which was placed in an enzyme marker and the 24 h growth curve was measured at OD_{600} nm.

The doubling time was calculated by linearly fitting the slope of the logarithmic phase of probiotic growth with the formula 1.

$$g = \frac{\ln 2}{k} \quad (1)$$

Where, g is the doubling time; k is the slope.

The activated probiotic bacteria were inoculated in polysaccharide-MRS medium and incubated at 37°C, 200 rpm incubator. After 24 h of fermentation, the bacterial solution was diluted to 10^{-6} dilution, 100 μL of the bacterial solution was inoculated in solid MRS medium and coated evenly with a coating stick, and they were incubated in an anaerobic incubator at 37°C for 24 h. The bacteria were counted by ImageJ. The calculation formula 2 was as follows.

$$N = \frac{C \times 10}{10^{-D}} \quad (2)$$

Where, N = CFU/mL; C = number of bacterial monoclonal; D = dilution multiple.

The configured MRS-protein medium was dispensed into 50 mL sterile centrifuge tubes, inoculated with 1% bacterial solution into the medium, incubated at 37°C and 200 rpm, and the bacterial solution was taken every 3 h. The pH value was measured using a pH meter.

2.5. Determination of the number of probiotic adherent colonies and the microscopic morphology of adherence

The probiotic adhesion model based on mouse intestinal tissues established in the previous laboratory was used to determine the adhesion ability of LP45 (Liu et al., 2022). Two intestinal segments co-cultured with LP45 were taken, one of which was added with 1 mL of 0.1 M phosphate buffer, and the intestinal tissues were cut into homogenates using sterile scissors and collected in sterile EP tubes for backup; the collected homogenates were diluted to 10^{-1}, 10^{-2}, 10^{-3} and 10^{-4}, and then take 10 μL of each coating plate; counted after 24 h of anaerobic incubation. The other intestinal segment was placed in a sterile 24-well plate and fixed with 2 mL of 2.5% (v/v) glutaraldehyde

for 4 h; washed three times with 0.1 M phosphate buffer (pH = 7.3); the intestinal segment was washed three times with distilled water at 4°C; freeze-dried for 18 h. The intestinal segment was placed on a short aluminum tube with double-sided adhesive, sputter-coated with pure gold, and then imaged by SEM to observe the microscopic morphology of the intestine. The magnification was 10, 000 × .

2.6. Measurement of adhesion-related indicators of the intestinal environment

Polysaccharide content determination: 200 μL of intestinal tissue homogenate was taken, and the change of polysaccharide content in the intestinal tissue model with adherent probiotics was determined by phenol sulfate method.

Biofilm assay: 200 μL of intestinal tissue homogenate was taken, 200 μL of 10 mg/L crystal violet was added and incubated for 15 min, the samples were washed three times with 0.01 M PBS, 1 mL of 95% (v/v) ethanol was added, 200 μL was transferred to a 96-well plate, and the absorbance at 570 nm was measured.

Determination of protein content: 200 μL of intestinal tissue homogenate was taken, and the changes of protein content in the intestinal tissue model with adherent probiotics were determined by the Coomassie Brilliant Blue G-250 method.

Determination of protein molecular weight: Take the intestinal tissue homogenate, add an appropriate amount of 5 × spiking buffer, heat it in a boiling water bath for 3–5 min, remove it, cool it, centrifuge it at 10, 000 rpm for 15 s, and take the supernatant as a backup. The changes of protein molecular weight in the intestinal tissue homogenate were analyzed by SDS-PAGE method.

2.7. Statistical analysis

All values were represented as mean ± SEM. Statistical analysis was carried out using PRISM 8.0 software. One-way analysis of variance (ANOVA) was adopted to compare the significant differences among all of groups. Differences were considered to be significant at $p < 0.05$.

3. Results

3.1. Physicochemical properties of IeP, SP and WP

The molecular weight size, amino acid composition and structural properties (microscopic morphology, secondary and tertiary structures, etc.) of proteins will directly determine the functional properties of proteins. IeP, SP, and WP represent different sources of dietary proteins, which are an important part of the human diet and are available from a wide range of sources, while the structural differences between different sources of food-derived proteins have rarely been studied.

As shown in Fig. 1A, the molecular weights of the three proteins were mainly distributed between 14.3 and 97.2 kDa, and there were large differences in the protein fractions, with obvious protein bands around 14.3, 20.1, 29.0, and 66.4 kDa for IeP, and the most obvious and darkest protein bands around 60 kDa, which accounted for a higher proportion of IeP. The molecular weight of SP was mainly distributed between 29.0 and 97.2 kDa, and there were distinct protein bands around 29.0, 66.4 and 97.2 kDa, with darker bands around 29 kDa–60 kDa. The molecular weights of IeP and SP were widely distributed with large molecular weights, while the molecular weights of WP were relatively small.

In order to understand the differences in the microscopic morphology of different food-derived proteins, the microstructures of three freeze-dried food-derived protein powders were observed by scanning electron microscopy (SEM), Fig. 1B,C,D shows the SEM images of IeP, SP, and WP at 1, 000 × magnification, respectively. As shown in the figures, IeP contains a variety of microscopic forms with different morphological proteins such as spherical, elongated, fibrous, etc. The structure is dense and inhomogeneous. Irregular spherical proteins with different sizes of folds can be seen under SEM in the form of spherical concave surfaces. Microscopic forms of WP show spherical proteins of different sizes, indicating smooth, spherical concave surfaces, which are unevenly aggregated into large spherical shapes. Collectively, IeP was found to be denser in structure and more complex in morphology.

As shown in Fig. 1E, from the infrared spectrogram, we can obtain information on the chemical bonds and functional groups contained in the food-derived protein molecules. Absorption peaks for IeP are found

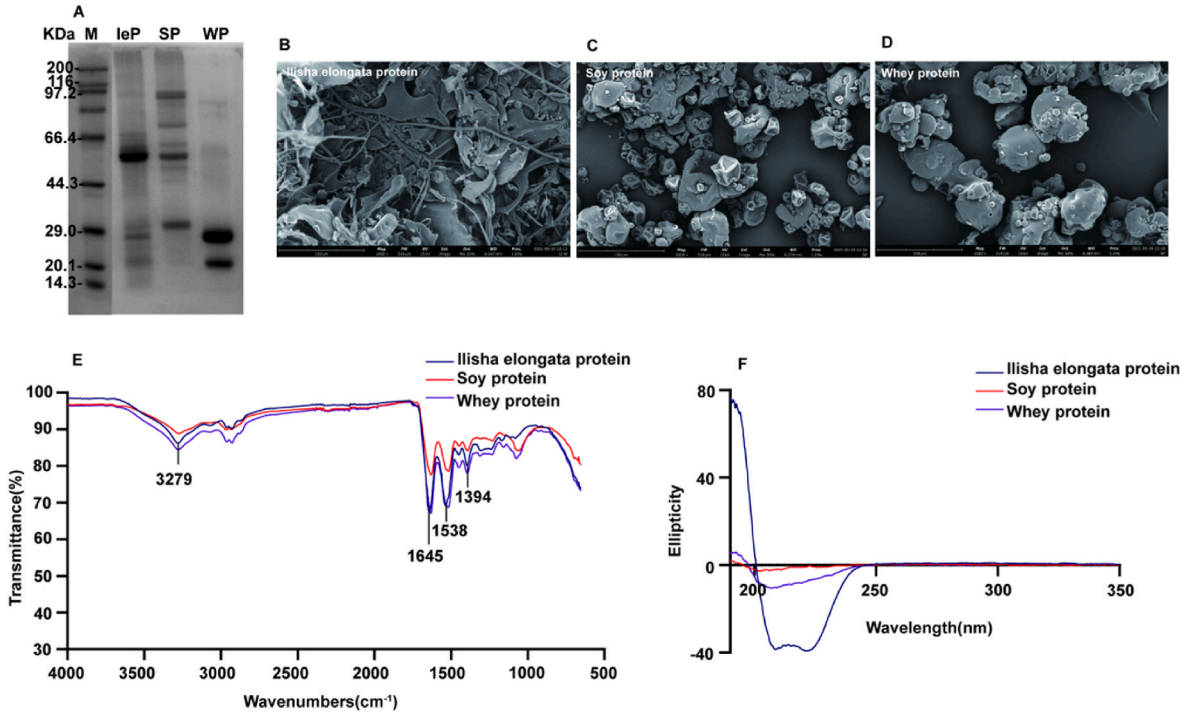

Fig. 1. Protein electrophoresis band (A); Scanning electron microscopy (B); Infrared spectroscopy (C); Circular dichroic graph (D).

at 3, 279 cm^{-1}, 1, 645 cm^{-1}, 1, 538 cm^{-1}, and 1, 394 cm^{-1}, indicating the stretching vibration of –OH, the stretching vibration of C═O in the amide I band, the bending vibration of N–H, and the bending vibration of –OH, respectively. The characteristic absorption peaks of –OH stretching vibration are 3276 cm^{-1} for both SP and WP, 1, 630 cm^{-1} for C═O stretching vibration in the amide I band, 1, 516 cm^{-1} for N–H bending vibration, and 1, 394 cm^{-1} for C–N stretching vibration in the amide II band, respectively. Comprehensive analysis reveals that the structures of SP and WP are similar, and IeP have smaller differences.

Fig. 1F shows the circular dichroism chromatograms of the three proteins, and the content of the protein secondary structures can be calculated. As shown in Table 1, the structure of IeP was mainly influenced by α-helix, β-fold and irregularly coiled structures with 38.53 ± 0.35%, 30.43 ± 1.20% and 30.53 ± 1.19%, respectively. The structure of SP was mainly influenced by β-fold and irregularly coiled structures with 43.67 ± 0.76% and 48.03 ± 0.42%, respectively. Hao et al. (Hao et al., 2013)used circular dichroism to measure that the secondary structure of soybean SP was mainly influenced by the β-fold and irregular curl structures with 60% and 32.3%, respectively, and that ultrasonic treatment altered the secondary structure of soybean SP. The structure of WP was mainly affected by the β-fold and irregular curl structures, with 44.20 ± 0.56% and 36.20 ± 0.62%, respectively.

3.2. Amino acid composition of IeP, SP and WP

As shown in Table 2, IeP, SP, and WP all had the same amino acid type but differed in content. The amino acid (AA) composition of the three food-derived proteins was higher in glutamic acid and aspartic acid, with glutamic acid and aspartic acid (17.02 g/100 g protein) and aspartic acid (12.62 g/100 g protein) in IeP, glutamic acid (19.49 g/100 g protein) and aspartic acid (11.63 g/100 g protein) in SP, glutamic acid (19.49 g/100 g protein) and aspartic acid (11.73 g/100 g protein), and glutamic acid (18.53 g/100 g protein) and aspartic acid (11.63 g/100 g protein) in WP. Food-derived proteins are rich in aspartic acid and glutamic acid, indicating the acidic character of these proteins, which are also known for their fresh tasting amino acids (Zhang et al., 2015). The essential amino acid (EAA) content of IeP, SP and WP was 44.49%, 43.59% and 48.03%, respectively, with WP having the highest EAA content. The EAA content and AA composition of dietary protein sources contribute to the different synthetic responses of muscle proteins to different protein intakes. The leucine content and EAA content of SP were relatively low compared to IeP and WP, whose EAA content remained at a high level compared to other dietary proteins, and the EAA content of tuna protein was 26.40% (Kim, 2021).

It has been found that plant proteins have relatively low levels of essential amino acids and leucine compared to animal proteins and human skeletal muscle proteins, resulting in reduced anabolic capacity of plant proteins (Shm et al., 2018). In contrast, co-administration of plant proteins with a multi-strain probiotic can increase postprandial changes in blood amino acids, which are closely associated with optimal muscle health. Probiotic supplementation could be an important nutritional strategy to overcome the deficiencies of plant protein composition (Jäger et al., 2020). The amino acid profile of food-derived proteins plays an important role in various biological and physiological activities and in the maintenance of human health. Amino acids such as aspartic acid, glycine and glutamic acid promote wound healing (Jong-Hee and Paul, 1984).

Table 1
Secondary structure content of protein.

Protein samples	α-helix(%)	β-folding(%)	β-turning angle (%)	Random coil (%)
IeP	38.53 ± 0.35[a]	30.43 ± 1.20[b]	0.60 ± 0.10[b]	30.53 ± 1.19[c]
SP	8.33 ± 0.38[c]	43.67 ± 0.76[a]	–	48.03 ± 0.42[a]
WP	13.33 ± 0.76[b]	44.20 ± 0.56[a]	6.50 ± 0.46[a]	36.20 ± 0.62[b]

Table 2
Amino acid composition and content of protein.

Amino acids(g/100g protein)	Amino acid type	IeP	SP	WP
Essential amino acids	Met	1.33	0.30	0.97
	Thr	4.89	4.12	7.88
	Val	5.3	4.35	5.41
	Ile	4.57	4.22	6.01
	Leu	9.41	7.86	10.89
	Phe	3.00	5.44	3.10
	Lys	8.36	6.58	10.18
	His	2.22	2.50	1.53
	Arg	5.41	8.22	2.06
Non-essential amino acids	Asp	12.62	11.73	11.63
	Glu	17.02	19.49	18.53
	Ser	4.68	5.48	5.04
	Gly	6.12	4.29	1.76
	Ala	9.70	4.24	5.22
	Cys-Cys	0.05	0.29	1.92
	Pro	2.59	5.63	2.48
	Tyr	2.72	3.90	3.18
	Total amino acids	97.27	94.74	94.61
	Essential amino acid	44.49	43.59	48.03

3.3. Growth and proliferation of LP45 by IeP, SP and WP

Probiotics rely on extracellular proteases to hydrolyze proteins into oligopeptides or amino acids, and then, the hydrolysis products are transported into the cell via the oligopeptide transport system (Opp), dipeptide transport system (DtpP), and tripeptide transport system (DtpT). DtpT preferentially transports hydrophobic dipeptides and tripeptides (Lopez-Kleine and Monnet, 2011). Finally, cleavage by various intracellular peptidases forms free amino acids for cellular synthesis and metabolism (Foucaud et al., 1995).

Fig. 2A shows the growth curves of LP45 in each experimental group, in which the final OD values of the three experimental groups with herring protein were similar to the final OD values of the MRS experimental group, and the growth time of LP45 was calculated according to the growth curve of LP45, as shown in Fig. 2B, the growth time of IeP, SP, and WP groups were significantly lower compared with the growth time of MRS experimental group, i.e., the growth period of LP45 was significantly shortened. The addition of 0.5 mg/mL and 1 mg/mL significantly reduced the growth time of LP45, and the addition of food-derived protein had less effect on the growth time of LP45.

The acid production ability of probiotic bacteria is one of their important growth characteristics, and the fermentation of probiotic bacteria produces large amounts of acid and lowers the pH, which can well inhibit the growth of other miscellaneous bacteria. Fig. 2C shows the changes of acid production capacity of different LP45 under different conditions of fermentation for 24 h. The initial pH of each medium was around 5.8, and the pH decreased continuously with the acid production by probiotic fermentation, and finally the pH reached around 3.8 after 24 h of fermentation. The effect of different food-derived proteins on the acid production capacity of LP45 was less, and the effect of unconcentrated proteins on the acid production capacity of LP45 was also less. Cao et al. (Cao et al., 2019) found that the effect of different oligosaccharides on the acid production capacity of LP45 was also less.

As shown in Fig. 2D, compared with MRS experimental group, IeP substituted peptone and IeP added experimental group significantly increased the total number of colonies of LP45, and the total number of colonies was positively correlated with the concentration of IeP added, where the MRS+1 mg/mL IeP experimental group had the highest total number of colonies, which was 2.385 × 10^{10} CFU/mL compared with MRS experimental group, SP substituted peptone Compared with the MRS experimental group, both the SP replacement peptone and SP addition experimental groups significantly increased the total number of

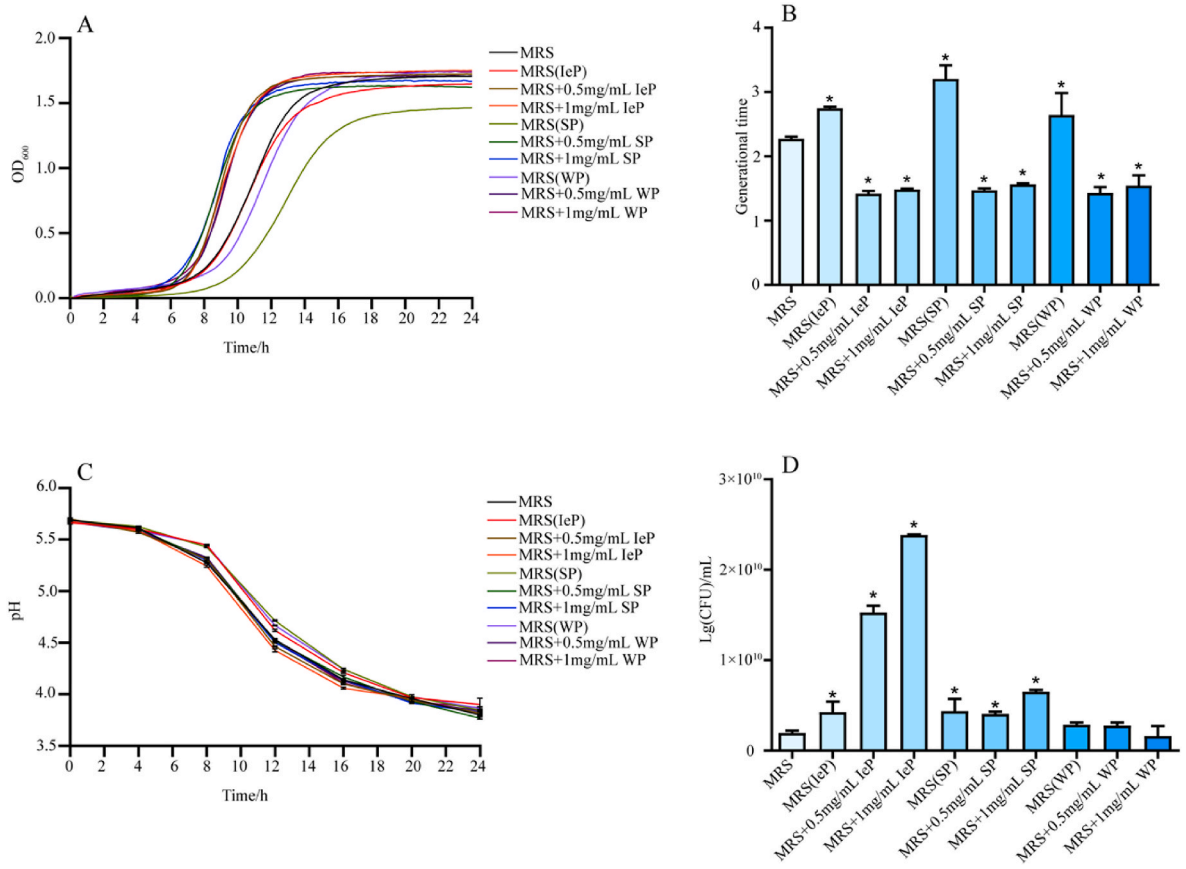

Fig. 2. Growth curve of LP45 (A); Growth generation of LP45 (B); Acid production capacity of LP45 (C); Total number of LP45 colonies (D); *$p < 0.05$, compared with the MRS group.

colonies of LP45, and the MRS+1 mg/mL SP experimental group had a relatively high total number of colonies, which was 6.5×10^9 CFU/mL. Compared with the MRS experimental group, the replacement and addition of WP had no significant effect on the total number of colonies of LP45.

3.4. Intestinal adhesion of LP45 by IeP, SP and WP

Adhesion is a complex process involving both non-specific (interactions between cell surfaces) and specific ligand-receptor interactions (Okochi et al., 2017). Hydrophobicity and autoaggregation abilities are important forces for probiotic bacteria to adhere to biotic or abiotic surfaces. Souza et al. (Souza et al., 2018) showed that bacteria with higher hydrophobicity could better bind to epithelial cells, thus affecting adhesion ability to some extent. The strength of bacterial surface hydrophobicity and self-aggregation ability depends mainly on the number of non-polar groups on the bacterial surface, and is related to the structure of surface proteins, bacterial hairs, lipophosphatidic acid, and podocytes (Remus et al., 2011), and strains with greater hydrophobicity have a greater ability to adhere (Giaouris et al., 2009). Self-aggregation of probiotic strains seems its necessary for adhesion to intestinal epithelial cells, while the co-aggregation ability may form a barrier against pathogenic microbial colonization. Co-aggregation of probiotics with intestinal pathogenic bacteria may allow easier elimination of pathogenic bacteria from the intestinal environment, while agglutination of Lactobacillus producing inhibitory substances with pathogenic bacteria helps the host to resist pathogenic infection (García-Cayuela et al., 2014).

Firstly, we evaluated how the adhesion capacity of LP45 changed with the addition of food-derived proteins by measuring the effects of different food-derived proteins on the hydrophobic capacity, self-aggregation capacity and copolymerization capacity of LP45 with pathogenic bacteria. As shown in Fig. 3, the results showed that the effect of IeP on the hydrophobic, self-aggregating and copolymerizing abilities of LP45 was small and not statistically significant. SP significantly decreased the hydrophobic ability of LP45, while significantly elevated its self-aggregating ability and decreased the copolymerizing ability. WP had a small effect on the hydrophobic and self-aggregating abilities of LP45, but decreased the copolymerizing ability. The adhesion capacity of probiotics is affected by several factors, and the effect of food-derived proteins on the hydrophobicity, self-aggregation capacity and copolymerization capacity of LP45 also affects its adhesion capacity to some extent.

Bacterial adhesion on the intestine occurs in a complex environment in vivo. In order to accurately evaluate the intestinal adhesion ability of bacteria and more realistically simulate the intestinal environment in vivo, we innovatively established the LP45 adhesion model based on mouse intestinal tissues. The number of live bacteria adhering to probiotic bacteria in the model is an important index that directly reflects the adhesion ability, as shown in Fig. 4B, LP45 has different adhesion ability in different intestinal segments. The effect of adding 1 mg/mL of food-derived protein on LP45 adhesion in different intestinal segments was somewhat different. In the duodenal segment, the addition of IeP significantly increased the number from 4.00×10^6 to 1.02×10^7 of adherent colonies of LP45 in the duodenum, the addition of SP significantly reduced the number of adherent colonies of LP45 in the duodenum, and the addition of WP also increased the number of adherent colonies of LP45 in the duodenum, but not significantly. In the jejunal segment, LP45 in the food-derived protein group increased the number of adherent colonies relative to LP45 in MRS culture, and in the ileum segment, LP45 in the food-derived protein group significantly decreased the number of adherent colonies relative to LP45 in MRS culture, and the

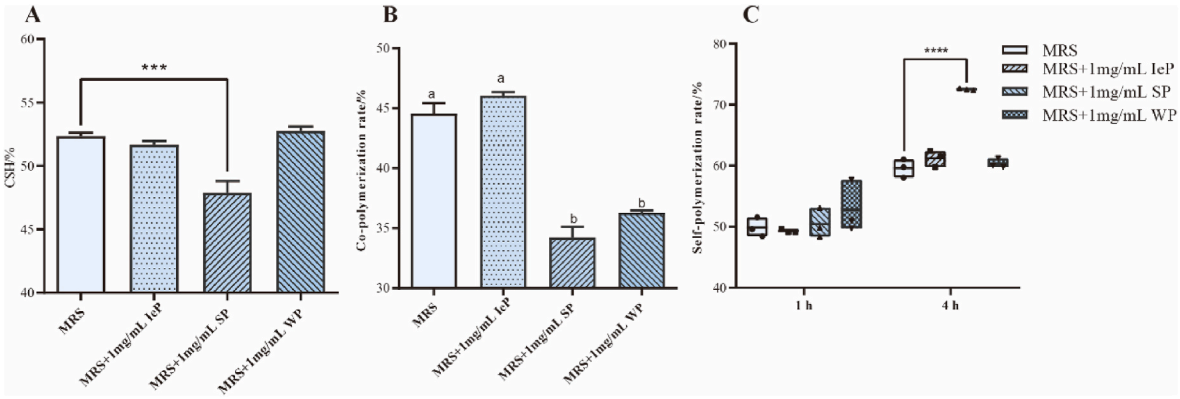

Fig. 3. Hydrophobicity of LP45 (A); Copolymerization capacity of LP45 (B); Self-aggregation of LP45 (C); *$p < 0.05$, compared with the MRS group.

number of adherent colonies in the IeP group was significantly greater than that in the SP and WP groups. In the cecum segment, the addition of IeP significantly reduced the number of adherent colonies of LP45 in the duodenum, and the addition of SP and WP increased the number of adherent colonies of LP45 in the duodenum, but it was not statistically significant. In the colonic segment, LP45 in the food-derived protein group significantly reduced the number of adherent colonies relative to LP45 in MRS culture, and the number of adherent colonies in the IeP group was significantly greater than that in the SP and WP groups, and the number of adherent colonies in LP45 cultured with the addition of IeP was 4.83×10^6. Taken together, the results showed that the addition of IeP culture significantly increased the number of adherent viable bacteria of LP45 on duodenum, SP significantly increased the number of adherent viable bacteria of LP45 on jejunum, while WP had no significant effect on the number of adherent viable bacteria of LP45 on each intestinal segment.

As shown in Fig. 4C, reflecting the adhesion of LP45 cultured with the addition of IeP, SP, and WP on each intestinal segment of mice photographed at 10, 000 × magnification by SEM, LP45 was observed to be tightly adhered to the surface of the intestinal mucosa in all groups, either encapsulated in a reticular structure of mucus or encapsulated in an extracellular polymer of probiotic bacteria. The IeP group could observe multiple organisms forming a biofilm adhering to the jejunal mucosa, and the WP group could observe LP45 undergoing dichotomy in the jejunal segment.

3.5. *Effect of IeP, SP and WP on intestinal environmental index changes caused by LP45*

The mucus layer of the gastrointestinal tract is a complex medium rich in glycoproteins, antimicrobial peptides, immunoglobulins and many other intestinal proteins, as well as lipids and electrolytes, and this layer constitutes a physical and chemical barrier between the intestinal contents and the underlying epithelium (Ermund et al., 2013). The gastrointestinal mucus is divided into an outer loose layer and an inner layer, and some studies have shown that bacteria are present only in the outer mucus layer, with probiotics adhering to the outer mucus layer (Juge, 2012). While the tightly layered inner mucus layer isolates the epithelial cells from the normal bacteria in the colonic lumen (Hansson and Johansson, 2008). The inner mucus layer is impermeable to bacteria and is 50–80 μm thick in mice and rats and approximately 100 μm thick in humans (Atuma et al., 2001; Gustafsson, 2011).

The adhesion of probiotics is closely related to the different structures and specific cell wall components, such as bacterial hairs or hair proteins, adhesins, lipoprotein, epithelial proteins, mucus binding proteins, fibronectin, extracellular polysaccharides, lipopolysaccharides, peptidoglycans and other components, which provide an advantage for probiotic colonization of the intestinal epithelium (Hynonen and Palva, 2013), Yong et al. (Yong and Klaenhammer, 2010) found that an aggregation promoting factor of Lactobacillus acidophilus NCFM deletion reduced adhesion to Caco-2 cells, mucins and laminin, but the morphology of bacterial cells was not altered. Recent studies showed that maturation and function of the mucus layer are strongly influenced by the gut microbiota. In return, the glycan repertoire of mucins can select for distinct mucosa-associated bacteria that are able to bind or degrade specific mucin glycans as a nutrient source (Schroeder, 2019).

The intestinal polysaccharide content reflected the changes in the content of extracellular polysaccharides secreted by probiotics and mucopolysaccharides degraded and utilized by probiotics, and Fig. 5A shows the changes in polysaccharide content caused by the adhesion of LP45 in each intestinal segment in different food-derived protein groups. As shown in the figure, in the duodenal segment, LP45 adhesion in the MRS and IeP groups significantly increased the intestinal polysaccharide content, and the intestinal polysaccharide content in the IeP group was significantly higher than that in the MRS group, and the intestinal polysaccharide content in the IeP group was 51.39 ± 0.36 μg/mm While LP45 adhesion in the SP and WP groups significantly decreased the intestinal polysaccharide content of. In the jejunal segment, LP45 adhesion significantly increased the intestinal polysaccharide content in all groups, and in the ileal segment, LP45 adhesion significantly increased the intestinal polysaccharide content in all groups except for the WP group, where LP45 adhesion significantly decreased the intestinal polysaccharide content. In the cecum segment, adhesion of LP45 in the MRS and WP groups significantly decreased the polysaccharide content in the intestine, while the IeP and SP groups significantly increased the polysaccharide content in the intestine. In the colonic segment, the intestinal polysaccharide content of all three food-derived protein groups was significantly higher than that of the MRS group. Taken together, these results revealed that IeP culture of LP45 contributed to its secretion of extracellular polysaccharides in the duodenum, jejunum, cecum and colon, SP culture of LP45 contributed to its secretion of extracellular polysaccharides in the jejunum, ileum, cecum and colon, and WP culture of LP45 contributed to its secretion of extracellular polysaccharides in the colon. The greater secretion of extracellular polysaccharides by LP45 in the intestine could more promote its adhesion in the intestine and improve the intestinal microenvironment. Extracellular polysaccharides may be involved in the biological activity of prebiotics and probiotics. Probiotic extracellular polysaccharides promote the formation of biofilm on the bacterial cell surface and can act as a protective barrier (Angelin and Kavitha, 2020).

Probiotic bacteria in biofilm-forming communities may be critical for long-term remodeling of the composition and beneficial function of the gut microbiome (Jones and Versalovic, 2009). As shown in Fig. 5B, in both the duodenal and jejunal segments, the adhesion of LP45 in all groups significantly reduced the biomass of intestinal biofilm. In the ileal segment, the intestinal biofilm biomass in the IeP group was

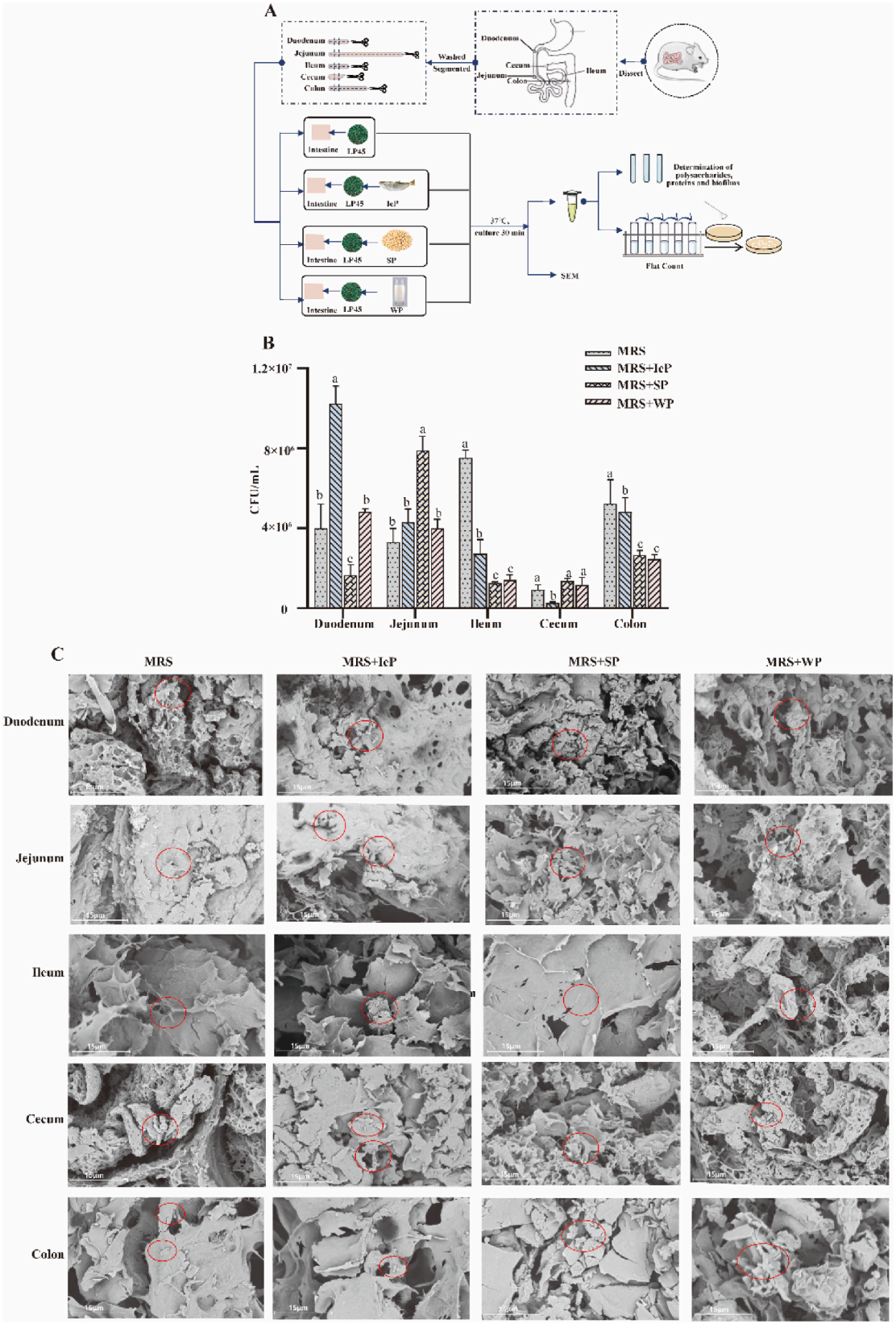

Fig. 4. Model diagram (A); Number of viable bacteria adhered to LP45 in intestinal tract (B); Electron microscopy of intestinal adhesion (C).

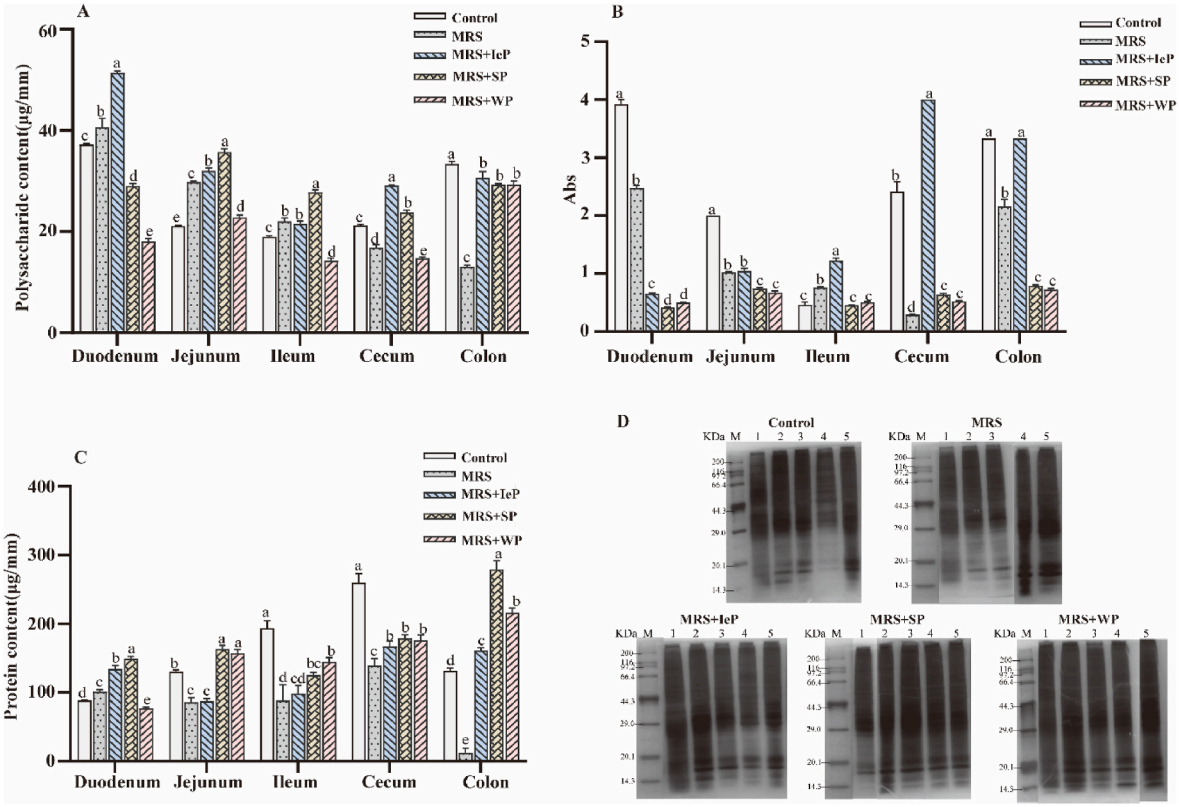

Fig. 5. Changes in sugar content in each intestinal segment (A); changes in biofilm biomass in each intestinal segment (B); changes in protein content in each intestinal segment (C); Protein molecular weight distribution of each intestinal segment (D).

significantly higher than that in the MRS group, and the intestinal biofilm biomass in the IeP group was 1.23 ± 0.04, while LP45 adhesion in the SP and WP groups had less effect on the intestinal biofilm biomass. In the cecum segment, the intestinal biofilm biomass was significantly higher only in the IeP group. In the colonic segment, the change in intestinal biofilm biomass was smaller in the IeP group, and the adhesion of LP45 significantly decreased the intestinal biofilm biomass in all other groups. The higher the ability of LP45 to form biofilm in the intestine, the more it promoted its adhesion in the intestine and its resistance to pathogenic bacteria.

The intestinal protein content reflects the changes in the content of adhesions such as surface proteins of probiotics, mucus in the intestine and intestinal microenvironment, and Fig. 5C shows the changes in protein content caused by the adhesion of LP45 in each intestinal segment in different food-derived protein groups. As shown in Fig. 5C, in the duodenal segment, the intestinal protein content in the IeP and SP groups was significantly higher than that in the MRS group, and the intestinal protein content in the IeP and SP groups were 134.65 ± 5.19 μg/mm and 149.49 ± 3.44 μg/mm, respectively. In the jejunal segment, LP45 adhesion in the SP-added and WP-added groups both significantly increased the intestinal. The protein content in the intestine was significantly increased in the SP and WP groups. In the ileal segment, the protein content in the ileum was significantly higher in the SP and WP groups compared with that in the MRS group. In the cecum, the intestinal protein content was significantly higher in the food-derived protein group compared with that in the MRS group in the cecum. In the colonic segment, adhesion of LP45 in the MRS group significantly decreased the intestinal protein content, while the intestinal protein content was significantly higher in both the food-derived protein groups, with the highest intestinal protein content of 279.52 ± 12.12 μg/mm in the SP group. Taken together, it was found that IeP culture of LP45 may contribute to the formation of mucin and stimulation of mucus secretion in the duodenum, cecum and colon, SP culture of LP45 contributes to the formation of mucin and stimulation of mucus secretion in various intestinal segments, and WP culture of LP45 contributes to the formation of mucin and stimulation of mucus secretion in the jejunum, ileum, cecum and colon. The formation of mucoadhesive in the intestine helps LP45 to colonize and survive in the intestine, and the secretion of mucus in the intestine is more conducive to the colonization of probiotics.

Fig. 5D shows the effects of IeP, SP, and WP on the molecular weight distribution of LP45 adhering to the duodenum, jejunum, ileum, cecum, and colon proteins. As shown in the figure, the intestinal tissues including intestinal epithelial cells intestinal mucus, which contains a wide variety and complexity of proteins, have more content of large molecular weight proteins, the distribution of small and medium molecular weight proteins in the electrophoresis pattern is relatively clear, the jejunum tissue has 3 clear protein bands between 14.3 and 20.1 kDa, and the ileum, cecum and colon tissues have 2 clear protein bands between 14.3 and 20.1 kDa. The cecum and colon tissues adhered by LP45 in the MRS group had 2 additional clear protein bands between 14.3 and 20.1 kDa. In contrast, LP45 adhesion in the three groups with food-derived protein added to the culture resulted in an increase of 2 clear protein bands between 14.3 and 20.1 kDa in each intestinal segment, with darker color and more small molecular weight protein content. Whereas mucins in mucus are large, highly glycosylated molecules composed of multiple subunits with a size range of 250–500 kDa (Rojas et al., 2002), the added bands exclude them from being mucins, and Christine et al. (Christine et al., 2010) found that an epi-protein with a molecular weight of 29.0 kDa released from Lactobacillus RC-14, which inhibits the adhesion of Enterococcus faecalis, is considered an adhesin. Then, the addition of two protein strips between 14.3 and 20.1 kDa may be an adhesin-associated protein of LP45, providing new speculations for subsequent studies such as food-derived proteins promoting the secretion of adhesins by LP45.

4. Conclusion

In this study, three different food-derived proteins were used to culture LP45, and the effects of IeP, SP and WP on the growth characteristics of LP45 such as growth generation time, total number of colonies and acid production capacity were compared. The results showed that the addition of 1 mg/mL IeP and SP significantly accelerated the growth rate of LP45 and significantly increased the total number of proliferating colonies, while the addition of 1 mg/mL WP only significantly accelerated the growth rate of LP45, and the addition of the three food-derived proteins had little effect on the acid production capacity of LP45. In this study, a probiotic adhesion model based on mouse intestinal tissues was used to evaluate the effects of IeP, SP and WP on the adhesion capacity and intestinal microenvironment of LP45 in each intestinal segment. The results showed that IeP significantly increased the number of LP45 adherent live bacteria in the duodenal segment, SP significantly increased the number of LP45 adherent live bacteria in the jejunal segment, and WP had less effect on the number of LP45 adherent live bacteria in each intestinal segment. The microenvironment of each intestinal segment was improved. Food-derived proteins also influenced the hydrophobicity, self-aggregation and copolymerization ability of LP45. The combined effect of food-derived proteins on probiotic provalue-added and increased adhesion capacity was found. Strongly suggesting that food-derived proteins promote intestinal health, showing their potential as active proteins.

CRediT authorship contribution statement

Guoyan Liu: Investigation, Methodology, Writing – original draft, Writing – review & editing. **Meng Chu:** Investigation, Formal analysis, Writing – original draft, Writing – review & editing. **Shiying Nie:** Writing – review & editing. **Xin Xu:** Resources. **Jiaoyan Ren:** Resources, Supervision, Project administration.

Declaration of competing interest

The authors declare that they have no known competing financial interests or personal relationships that could have appeared to influence the work reported in this paper.

Acknowledgments

This research was supported by funds from the National Key R&D Program of China, China (2018YFD0901101).

References

Alp, D., Kuleaşan, H., 2019. Adhesion mechanisms of lactic acid bacteria: conventional and novel approaches for testing. World J. Microbiol. Biotechnol. 35 (10), 156. https://doi:10.1007/s11274-019-2730-x.

Angelin, J., Kavitha, M., 2020. Exopolysaccharides from probiotic bacteria and their health potential. Int. J. Biol. Macromol. 162, 853–865. https://doi:10.1016/j.ijbiomac.2020.06.190.

Atuma, C., Strugala, V., Allen, A., Holm, L., 2001. The adherent gastrointestinal mucus gel layer: thickness and physical state in vivo. Am. J. Physiol. Gastrointest. Liver Physiol. 280 (5), G922. https://doi:10.1152/ajpgi.2001.280.5.G922.

Cao, P., Wu, L., Wu, Z., Pan, D., Zeng, X., Guo, Y., et al., 2019. Effects of oligosaccharides on the fermentation properties of lactobacillus plantarum. J. Dairy Sci. 236 (1), 2863–2872. https://doi:10.3168/jds.2018-15410.

Christine, H., Van, H.V.J.E.T., Janssen, D.B., Busscher, H.J., Vander, M.H.C., Gregor, R., 2010. Purification and characterization of a surface-binding protein from lactobacillus fermentum rc-14 that inhibits adhesion of enterococcus faecalis 1131. FEMS Microbiol. Lett. (1), 177–180. https://doi:10.1111/j.1574-6968.2000.tb09282.x.

Deng, Y., Huang, L., Zhang, C., Xie, P., Cheng, J., Wang, X., et al., 2019. Physicochemical and functional properties of Chinese quince seed protein isolate. Food Chem. 283, 539–548. https://doi.org/10.1016/j.foodchem.2019.01.083.

Ermund, A., Schutte, A., Johansson, M.E.V., Gustafsson, J.K., Hansson, G.C., 2013. Studies of mucus in mouse stomach, small intestine, and colon. i. gastrointestinal mucus layers have different properties depending on location as well as over the peyer's patches. AJP Gastrointestinal and Liver Physiology 305 (5), G341–G347. https://doi:10.1152/ajpgi.00046.2013.

Foucaud, C., Kunji, E.R., Hagting, A., Richard, J., Konings, W.N., Desmazeaud, M., et al., 1995. Specificity of peptide transport systems in lactococcus lactis: evidence for a third system which transports hydrophobic di- and tripeptides. J. Bacteriol. 177, 4652–4657. https://doi:10.1128/jb.177.16.4652-4657.1995.

García-Cayuela, T., Korany, A.M., Bustos, I., Cadiñanos, L., Requena, T., Peláez, C., et al., 2014. Adhesion abilities of dairy lactobacillus plantarum strains showing an aggregation phenotype. Food Res. Int. 57, 44–50. https://doi:10.1016/j.foodres.2014.01.010.

Gentile, C.L., Weir, T.L., 2018. The gut microbiota at the intersection of diet and human health. Science 362 (6416), 776–780. https://doi:10.1126/science.aau5812.

Giaouris, E., Chapot-Chartier, M.P., Briandet, R., 2009. Surface physicochemical analysis of natural lactococcus lactis strains reveals the existence of hydrophobic and low charged strains with altered adhesive properties. Int. J. Food Microbiol. 131 (1), 2–9. https://doi:10.1016/j.ijfoodmicro.2008.09.006.

Gustafsson, J.K., 2011. An ex vivo method for studying mucus formation, properties, and thickness in human colonic biopsies and mouse small and large intestinal explants. Am. J. Physiol. Gastrointest. Liver Physiol. 302 (4), G430. https://doi:10.1152/ajpgi.00405.2011.

Hansson, G.C., Johansson, M.E., 2008. The inner of the two muc2 mucin-dependent mucus layers in colon is devoid of bacteria. Gut Microb. 105 (1), 51–54. https://doi:10.1073/pnas.0803124105.

Han, S., Lu, Y., Xie, J., Fei, Y., Li, L., 2021. Probiotic gastrointestinal transit and colonization after oral administration: a long journey. Front. Cell. Infect. Microbiol. 11 (1), 609722. https://doi:10.3389/fcimb.2021.609722.

Hao, H., Wu, J., Li-Chan, E., Le, Z., Fang, Z., Xu, X., et al., 2013. Effects of ultrasound on structural and physical properties of soy protein isolate (SPI) dispersions. Food Hydrocolloids 30 (2). https://doi:10.1016/j.foodhyd.2012.08.001.

Hynonen, U., Palva, A., 2013. Lactobacillus surface layer proteins: structure, function and applications. Appl. Microbiol. Biotechnol. 97 (12), 5225–5243. https://doi:10.1007/s00253-013-4962-2.

Jäger, R., Zaragoza, J., Purpura, M., Iametti, S., Taylor, L., 2020. Probiotic administration increases amino acid absorption from plant protein: a placebo-controlled, randomized, double-blind, multicenter, crossover study. Probiotics and Antimicrobial Proteins 8 (12), 1330–1339. https://doi:10.1007/s12602-020-09656-5.

Jones, S.E., Versalovic, J., 2009. Probiotic lactobacillus reuteri biofilms produce antimicrobial and anti-inflammatory factors. BMC Microbiol. 9 (1), 35-35. https://doi:10.1186/1471-2180-9-35.

Jong-Hee, C., Paul, G., 1984. Improvement of nitrogen retention by arginine and glycine supplementation and its relation to collagen synthesis in traumatized mature and aged rats. J. Nutr. 114 (9), 1697–1704. https://doi:10.1093/jn/114.9.1697.

Juge, N., 2012. Microbial adhesins to gastrointestinal mucus. Trends Microbiol. 20 (1), 30–39. https://doi:10.1016/j.tim.2011.10.001.

Juillard, V., Bars, D.L., Kunji, E., Konings, W.N., Richard, J., 1995. Oligopeptides are the main source of nitrogen for lactococcus lactis during growth in milk. Appl. Environ. Microbiol. 61 (8), 3024. https://doi:10.1002/bit.260470314.

Kim, S.K., 2021. Muscle protein hydrolysates and amino acid composition in fish. Mar. Drugs 19 (7), 377. https://doi:10.3390/md19070377.

Liu, G.Y., Chu, M., Xu, P., Nie, S.Y., Xu, X., Ren, J.Y., 2022. Effects of Ilisha elongata protein on proliferation and adhesion of Lactobacillus plantarum. Food Chem.: X, 2022 13, 100206. https://doi.org/10.1016/j.fochx.2022.100206.

Lopez-Kleine, L., Monnet, V., 2011. Lactic Acid Bacteria | Proteolytic Systems, second ed. Encyclopedia of Dairy Sciences, pp. 49–55 https://doi:10.1016/B978-0-12-374407-4.00257-0.

Mastrocola, R., Ferrocino, I., Liberto, E., Chiazza, F., Cento, As, et al., 2018. Fructose liquid and solid formulations differently affect gut integrity, microbiota composition and related liver toxicity: a comparative in vivo study. J. Nutr. Biochem. 55, 185–199. https://doi:10.1016/j.jnutbio.2018.02.003.

Okochi, M., Sugita, T., Asai, Y., Tanaka, M., Honda, H., 2017. Screening of peptides associated with adhesion and aggregation of lactobacillus rhamnosus GG in vitro. Biochem. Eng. J. 128, 178–185. https://doi:10.1016/j.bej.2017.10.004.

Pritchard, G.G., Tim, C., 1993. The physiology and biochemistry of the proteolytic system in lactic acid bacteria. FEMS Microbiol. Rev. (1–3), 179–206. https://doi:10.1016/0168-6445(93)90063-F.

Remus, D.M., Kleerebezem, M., Bron, P.A., 2011. An intimate tête-à-tête — how probiotic lactobacilli communicate with the host. Eur. J. Pharmacol. 668 (Suppl. S1), S33–S42. https://doi:10.1016/j.ejphar.2011.07.012.

Rojas, M., Ascencio, F., Conway, P.L., 2002. Purification and characterization of a surface protein from lactobacillus fermentum 104r that binds to porcine small intestinal mucus and gastric mucin. Appl. Environ. Microbiol. 68 (5), 2330–2336. https://doi:10.1128/AEM.68.5.2330-2336.2002.

Schroeder, B.O., Birchenough, G., Ståhlman, M., Arike, L., Johansson, M., Hansson, G.C., et al., 2017. Bifidobacteria or fiber protects against diet-induced microbiota-mediated colonic mucus deterioration. Cell Host Microbe 10 (1), 27–40. https://doi:10.1016/j.chom.2017.11.004.

Schroeder, B.O., 2019. Fight them or feed them: how the intestinal mucus layer manages the gut microbiota. Gastroenterology Report 1 (1), 1–10. https://doi:10.1093/gastro/goy052.

Shm, G., Jjr, C., Jmg, S., Wah, W., Bierau, J., Verdijk, L.B., et al., 2018. Protein content and amino acid composition of commercially available plant-based protein isolates. Amino Acids 50 (12), 1685–1695. https://doi:10.1007/s00726-018-2640-5.

Shoaie, S., Ghaffari, P., Kovatcheva-Datchary, P., Mardinoglu, A., Sen, P., Pujos-Guillot, E., et al., 2015. Quantifying diet-induced metabolic changes of the human gut microbiome. Cell Metabol. 22 (2), 320–331. https://doi:10.1016/j.cmet.2015.07.001.

Souza, B.D., Borgonovi, T.F., Casarotti, S.N., Todorov, S.D., Penna, A., 2018. Lactobacillus casei and lactobacillus fermentum strains isolated from mozzarella cheese: probiotic potential, safety, acidifying kinetic parameters and viability under gastrointestinal tract conditions. Probiotics & Antimicrobial Proteins 11, 382–396. https://doi:10.1007/s12602-018-9406-y.

Thomas, C.M., Versalovic, J., 2014. Probiotics-host communication. Gut Microb. (3), 148–163. https://doi:10.4161/gmic.1.3.11712.

Yong, J.G., Klaenhammer, T.R., 2010. Functional roles of aggregation-promoting-like factor in stress tolerance and adherence of *lactobacillus acidophilus NCFM*. Appl. Environ. Microbiol. 76 (15). https://doi:10.1128/AEM.00030-10.

Zhang, C., Zhang, Y., Li, H., Liu, X., 2020. The potential of proteins, hydrolysates and peptides as growth factors for lactobacillus and bifidobacterium: current research and future perspectives. Food Funct. 11. https://doi:10.1039/C9FO02961C.

Zhang, Q.L., Ren, J.Y., Zhao, H.F., Zhao, M.M., Xu, J.Y., Zhao, Q.Z., 2011. Influence of casein hydrolysates on the growth and lactic acid production of. Lactobacillus delbrueckii subsp. bulgaricus and Streptococcus thermophilus 46 (5), 1014–1020. https://doi.org/10.1111/j.1365-2621.2011.02578.x.

Zhang, Y., Zhao, W., Yang, R., 2015. Steam flash explosion assisted dissolution of keratin from feathers. ACS Sustain. Chem. Eng. 3 (9), 150717112248006. https://doi:10.1021/acssuschemeng.5b00310.